Electronic Supplementary Information

Composition and morphology tuning during hydrothermal synthesis of $Sr_xBa_{1-x}Nb_2O_6$ tetragonal tungsten bronzes studied by in situ X-ray diffraction

Ola G. Grendal [1], Anders B. Blichfeld [1], Tuong D. Vu [1], Wouter van Beek, [2] Sverre M. Selbach [1], Tor Grande [1] and Mari-Ann Einarsrud [1,*]

[1] Department of Materials Science and Engineering, NTNU Norwegian University of Science and Technology, 7491 Trondheim, Norway.
[2] Swiss-Norwegian Beamlines at European Synchrotron Research Facility, 38043 Grenoble, France.
* Correspondence: mari-ann.einarsrud@ntnu.no; Tel.: +47-735-94-002

Selected temperature profiles

Temperature profiles during heating of the capillary were measured with a thermocouple placed inside the sapphire capillary, while the capillary was filled with water and pressurized to 100 bar. Temperature profiles were measured in 50 °C intervals from 100 to 400 °C (referring to the set-point temperature of the heat blower). The measured values were then used to calibrate the set-point temperature of the heat blower with the actual temperature inside the capillary.

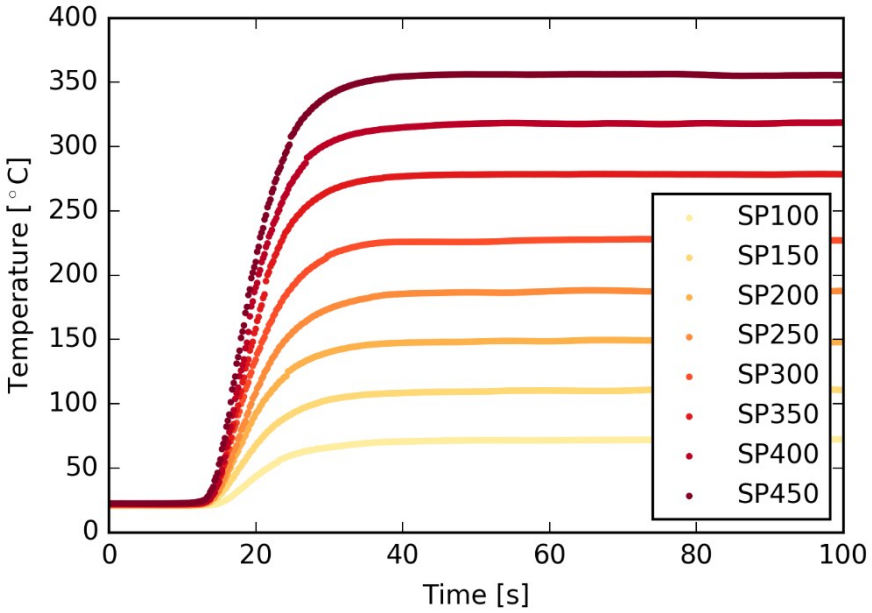

Figure S1: Heating profiles for various set-point temperatures (100 – 450 °C). For all set-point temperatures a steady state is reached after about 20 s.

Typical input file used for the sequential Rietveld refinement in *TOPAS*

For the sequential refinements the following parameters where refined for SBN: scale factor, two lattice parameters (a and c in the tetragonal cell), Lorentzian and Gaussian strain parameter, isotropic atomic displacement parameter (APD, Biso) for both the niobium and the alkaline earth sites (4 in total), Sr fraction, Sr occupancy on the A1-site and 3 atomic position parameters (in total 14 structural parameters). The 3 atomic position parameters were the x and y positions for the B2- and A1-site respectively (only one parameter is needed for the A1-site due to symmetry constraints). Sr was allowed to occupy the A1- and A2-sites, while Ba was locked to the A2-sites while keeping the stoichiometry (the sum of Ba and Sr equal to 5 plus 1 vacancy) and having physically meaningful occupancies (non-negative and not higher than 1). Ba was locked to the A2-site to avoid parameter correlation during refinement. The background was fitted with a 35th order Chebyshev polynomial to account for the broad background peak of water and solutes for each frame. Zero-shift error was refined for the last frame for each experiment, and then kept fixed for the sequential refinement. Atomic positions and B_{iso} values for all oxygen atoms were kept fixed to RT neutron data from Carrio et al. [1]. Because of the temperature being higher than, or close to the reported T_c for SBN for all experiments, the centrosymmetric space group (no. 127, *P4/mbm*) was used for all refinements instead of the reported non-centrosymmetric space group (no. 100, *P4bm*) stable at RT.

Below is a typical input-file for *TOPAS* used in this work, showing what equations and constraints are used for the different parameters. A "summarized" version of the input-file is presented in Table S1, and a typical graphical representation of a Rietveld refinement is presented in Figure S2.

```
r_exp  0.0255204487 r_exp_dash  0.127019401 r_wp  1.96483467 r_wp_dash  9.77929996 r_p  0.943879931 r_p_dash  9.91316111
weighted_Durbin_Watson  0.267602062 gof  76.9906006

iters 100000

xdd "IN_FILE.xye"

r_exp  0.0255204487 r_exp_dash  0.127019401 r_wp  1.96483467 r_wp_dash  9.77929996 r_p  0.943879931 r_p_dash  9.91316111
weighted_Durbin_Watson  0.267602062 gof  76.9906006

x_calculation_step 0.01

'35th order Chebychev

bkg @  22599.4817`_28.5226096 -20712.2473`_53.3728287  1593.86128`_51.3664193 -233.598229`_49.7733623  251.054531`_48.0132791 -
1755.78153`_46.9298452  2685.7828`_46.1299153 -898.431397`_45.0653321 -683.825704`_44.2134599  1284.87657`_43.7297047 -
409.724229`_43.2107424 -555.518095`_42.4263143  589.952675`_42.0875049 -144.851875`_41.3547231 -225.389735`_40.8036582
317.795294`_40.4192511 -107.279117`_39.9558045  76.0631089`_39.3158164  142.786448`_39.0693042  12.5318361`_38.460597
18.3369476`_38.1103801  78.7237282`_37.559452  48.0405916`_37.1906964 -3.35622708`_36.2257427 -17.0849808`_35.9528332
95.0641312`_35.110942 -24.0283942`_34.7009036  6.4279789`_33.1029892 -32.3078696`_32.356327  4.36366726`_30.2236073 -
22.5049771`_29.6072912 -14.1927031`_26.7415948  8.22815171`_25.0805855  21.8396967`_19.287633 -20.3509081`_15.112047

start_X  3

finish_X  51

no_LIMIT_warnings

do_errors

Zero_Error(!zero ,-0.00549`_0.00032)

lam ymin_on_ymax 0.001 la 1.0 lo 0.77445 lh 0.1

LP_Factor( 90) 'change the LP correction  or lh value if required
```

```
str

    e0_from_Strain( 0.00063`_0.00001, sgc, 0.23848`_0.00481, slc, 0.08791`_0.00518) 'defines and refines the values e0, name for Strain_G, value, name for Strain_L, value

    prm !e0_SBN =Voigt_FWHM_GL(CeV_or_0(sgc, sgv), CeV_or_0(slc, slv)) .25 Pi/360; :  0.00063`_0.00001 'calculates the e0 using a macro in topas.inc

    r_bragg r_b_SBN  1.11129852

    phase_MAC  22.296247`_0.0920996971

    phase_name "SBN"

    MVW( 1995.992`_2.409, 626.224`_0.024, 100.000`_0.000)

    scale scale_SBN  0.000309860911`_1.918e-006

    space_group P4/mbm

    Phase_LAC_1_on_cm( 118.00760`_0.62990)

    Phase_Density_g_on_cm3( 5.29271`_0.00639)

    Tetragonal(a_SBN  12.564880`_0.000213 min=12.45; max=12.60;, c_SBN  3.966552`_0.000076 min=3.955; max=3.98;)

    site Nb1 num_posns  2 occ Nb  1 beq b_Nb1  3.12544`_0.08979 min 0 max 7 x  0 y  0.5 z 0

    site Nb2 num_posns  8 occ Nb  1 beq b_Nb2  2.21513`_0.04540 min 0 max 7 x = 0.07529+xNb2; y = 0.21097+yNb2; z 0

    site A1 num_posns  2 x  0          y  0 z 0.5

            occ Sr  SrA1  0.92471`_0.01099 min = 1/2; max = Sr/2; beq b_A1  2.30362`_0.15923 min 0 max 7

    site A2 num_posns  4              x xA2 = 0.17097+disp;          y yA2 = 0.67097+disp;          z  0.5

            occ Sr  SrA2 =         (Sr-2*SrA1)/4; :  0.03903`_0.01330 beq b_A2  4.38415`_0.10159 min 0 max 7

            occ Ba  BaA2 =         Ba/4; :  0.74862`_0.01212          beq b_Ba2 = b_A2;

    site O1     num_posns  8 occ O   1 beq   1.90            x  0.3413   y  0.0055   z  0.0

    site O2     num_posns  8 occ O   1 beq   1.93            x  0.1413   y  0.0647   z  0.0

    site O3     num_posns  4 occ O   1 beq   0.13            x  0.2817   y  0.7817   z  0.0

    site O4     num_posns  2 occ O   1 beq   3.85            x  0                    y  0.5                    z  0.5

    site O5     num_posns  8 occ O   1 beq   2.88            x  0.2965   y  0.4175   z  0.5

    prm Sr  2.00554`_0.04846 min 1 max  4

    prm Ba = 5-Sr; :  2.99446`_0.04846

    prm disp  0.00229`_0.00017 min -0.01 max  0.01

    prm xNb2 -0.00090`_0.00014 min -0.01 max  0.01 'Dispplacment in x-direction for Nb2-site

    prm yNb2  0.00254`_0.00015 min -0.01 max  0.01 'Displcament in y-direction for Nb2-siter

    prm !sumA1 = SrA1; :  0.92471`_0.01099 'Total occupancy on A1 site

    prm !sumA2 = BaA2+SrA2; :  0.78765`_0.00549 'Total occupancy on A2 site

    prm !vac_A1 = (1-sumA1)*2; :  0.15059`_0.02197 'Fraction vacancy on A1

    prm !vac_A2 = (1-sumA2)*4; :  0.84941`_0.02197 'Fraction vacancy on A2

    prm !sum_vac = vac_A1+vac_A2; :  1.00000`_0.00000 'Total vacancy

    prm !sum_Ba = 4*BaA2; :  2.99446`_0.04846 'Total Ba
```

```
            prm !sum_Sr = 2*SrA1+4*SrA2; :  2.00554`_0.04846 'Total Sr
            prm !ratio_Sr = sum_Sr/(sum_Sr+sum_Ba); :  0.40111`_0.00969 'Amount of Sr in formula SrxBa1-xNb2O6
   TCHZ_Peak_Type(, -0.45497, ,-0.01050, , -0.45190, , 0.45791, , 0.00012, , 0.00182)
Out_X_Yobs_Ycalc_Difference("IN_FILE.txt")
            out "SBN_50_T300_P200.txt" append
            Out(Get (r_wp), "%.5e")
            Out(Get (r_exp), "%15.5e")
            Out(Get (gof), "%15.5e")
            Out(r_b_SBN, "%15.5e")
            Out(scale_SBN, "%15.5e", "%15.5e")
            Out(a_SBN, "%15.5e", "%15.5e")
            Out(c_SBN, "%15.5e", "%15.5e")
            Out(e0_SBN, "%15.5e", "%15.5e")
            Out(b_Nb1, "%15.5e", "%15.5e")
            Out(b_Nb2, "%15.5e", "%15.5e")
            Out(xNb2, "%15.5e", "%15.5e")
            Out(yNb2, "%15.5e", "%15.5e")
            Out(b_A1, "%15.5e", "%15.5e")
            Out(b_A2, "%15.5e", "%15.5e")
            Out(disp, "%15.5e", "%15.5e")
            Out(vac_A1, "%15.5e", "%15.5e")
            Out(sumA1, "%15.5e", "%15.5e")
            Out(sumA2, "%15.5e", "%15.5e")
            Out(ratio_Sr, "%15.5e", "%15.5e")
            Out(scale_pyro, "%15.5e")
            Out(zero, "%15.5e\n")
```

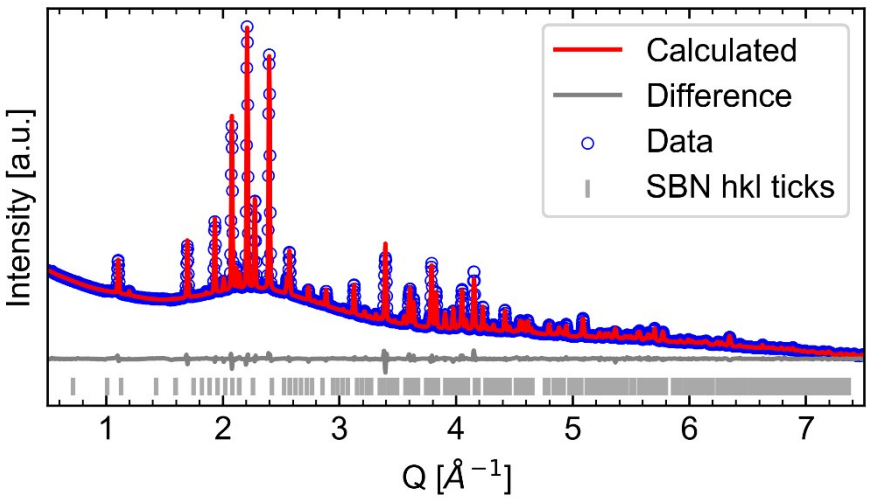

Figure S2: Representative graphical representation of a Rietveld refinement, presented with SBN50_T300 at the end of experiment.

Table S1. Overview of refined parameters from the Rietveld batch refinements and as preparation for the batch refinements respectively. Also included is a comment on what constraints or restrictions have been used for the different refinements.

Parameter	Prep refinement	Batch refinement	Comment
Zero error	Refined	Fixed	Fixed to value at end of experiment
Scale factor	Refined	Refined	
a [Å]	Refined	Refined	
c [Å]	Refined	Refined	
Gaussian and Lorentzian strain	Refined	Refined	
Sr fraction [a.u.]	Refined	Refined	
Sr occupancy A1 [a.u.]	Refined	Refined	
Sr occupancy A2 [a.u.]	Calculated	Calculated	Assuming unfilled TTB
Ba fraction [a.u.]	Calculated		Assuming Ba = 1 - Sr
Ba occupancy A1	Locked to 0		
Ba occupancy A2	Calculated		Assuming unfilled TTB
Nb2 atomic positions (x and y)	Refined	Refined	2 parameters
A1 atomic positions (x and y)	Refined	Refined	1 parameter (symmetry constraint)
O positions	Fixed	Fixed	Fixed to neutron data
O thermal parameters	Fixed	Fixed	Fixed to neutron data
Total parameters refined	15	14	

Validation of the Rietveld refinement model

$Sr_xBa_{1-x}Nb_2O_6$ (SBN100*x) was prepared by Aamlid et al. [2] by solid-state synthesis at 1400 °C with four different nominal compositions (SBN25_T800, SBN33_T800, SBN50_T800 and SBN61_T800) and synchrotron X-ray powder diffraction data was collected at SNBL, ESRF (λ = 0.77624 Å). Details of synthesis and X-ray diffraction measurements conditions are found in [2]. The same Rietveld refinement model as previously described was used on this data set to verify that especially the refined Sr fraction values can be trusted. Figure S3 shows the Rietveld refinements, and in Figure S4 the refined lattice parameters (a and c) are plotted as a function of refined Sr fraction (diamonds) and nominal Sr fraction (upside down triangle) and compared to literature values. The results show that the refined Sr fraction definitely can be trusted (refined lattice parameters as a function of refined Sr fraction fits well with literature). It is also observed that the refined Sr fractions are seemingly underestimating the nominal Sr fraction (this is assumed to be the real Sr fraction, since the samples are made by solid-state synthesis), as is seen by the better fit of the lattice parameters with literature when plotted versus the nominal Sr fraction.

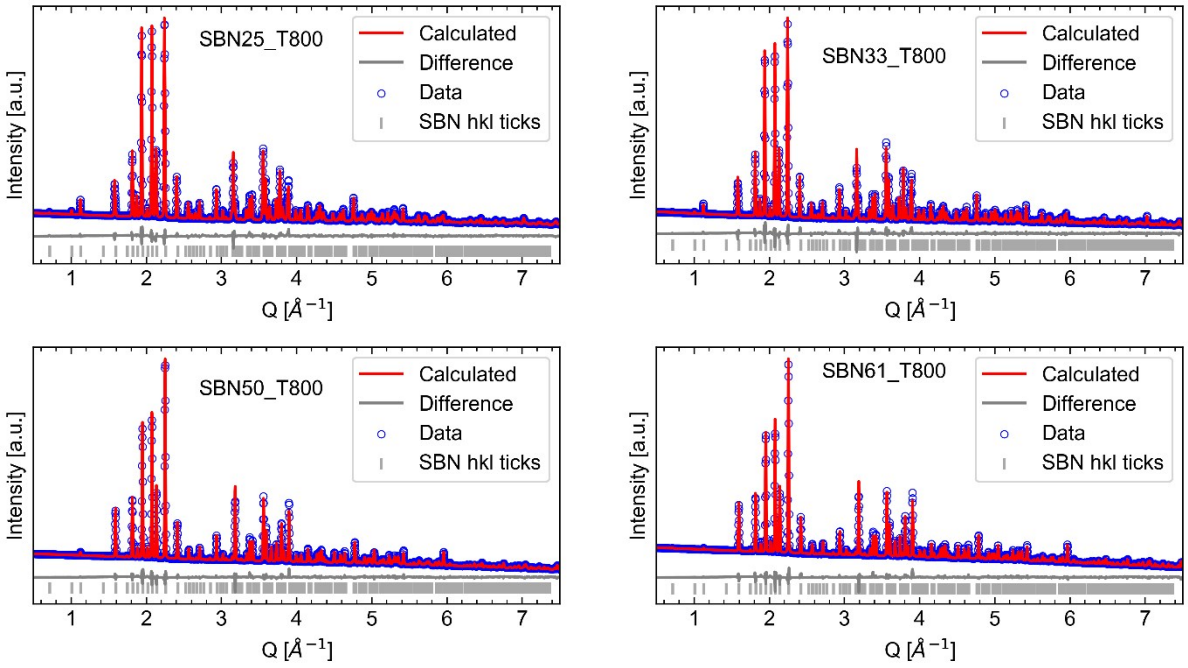

Figure S3: Rietveld refinement of SBN25_T800, SBN33_T800, SBN50_T800 and SBN61_T800 showing data (blue circles), calculated (red) and the difference between data and calculated (grey). Grey bars show theoretical hkl positions of the SBN diffraction lines.

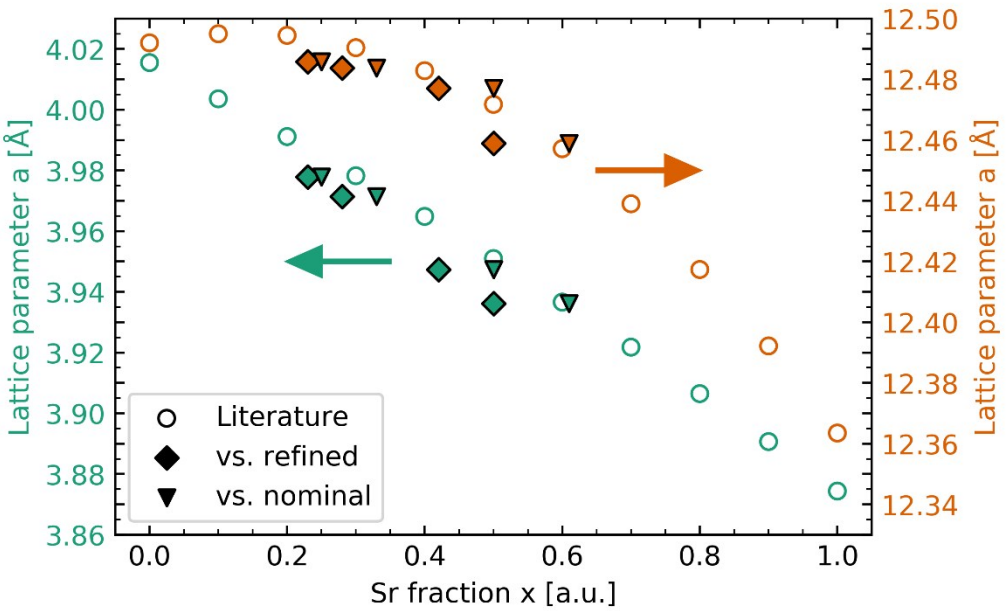

Figure S4: Refined lattice parameters for SBN (a and c) plotted versus refined Sr fraction (diamonds) and nominal Sr fraction (triangles). Indicated with open symbols are literature values for the a and c parameters at room temperature obtained from Podlozhenov et al. [3].

TEM study of observed rods and bipyramids from hydrothermal synthesis of SBN

A hydrothermal reaction was done in a conventional steel autoclave with a PTFE liner with a filling factor of 70 %. The reaction was performed at 250 °C for 48 h and a Sr fraction of 0.5 in the precursor. The X-ray diffraction pattern showed SBN as the main phase with traces of the Pyro phase. By scanning electron microscopy (SEM) a mixture of rods and bipyramids were observed. It was assumed that SBN had formed rods, while the Pyro phase formed bipyramids. To verify this transmission electron microscopy (TEM) with a combination of imaging, electron diffraction and energy-dispersive X-ray spectroscopy (EDX) were used.

A JEOL JEM-2100 TEM equipped with an Oxford X-max80 EDX-detector was used, with an acceleration voltage of 200 kV. The sample was prepared by dropping a diluted acetone-dispersion of the sample on a carbon coated copper TEM grid and let dry it dry for approximately 10 min.

The results show that the rods are in fact SBN, and that the bipyramids are Pyro. Also, it shows that the Pyro phase is Sr rich compared with the SBN rods.

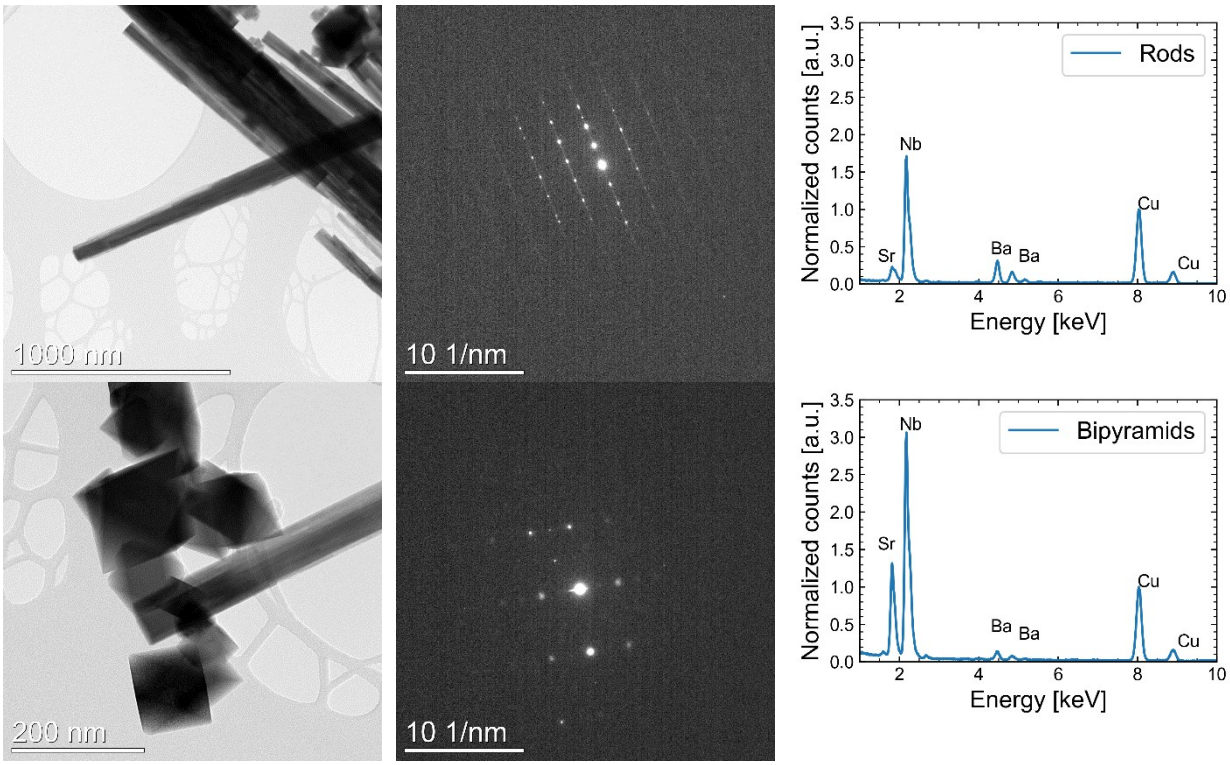

Figure S5: TEM images, electron diffraction and EDX for the observed rods (top row) and bipyramids (bottom row). EDX data are normalized to the most intense Cu-peak which is coming from the sample holder and is thus assumed to be comparable for the two EDX patterns.

Lattice parameters (a and c) from Rietveld refinement

Figure S6 shows lattice parameters *a* (a and b) and *c* (c and d) obtained from Rietveld refinement at the of the experiments plotted versus reaction temperature (a and c) and Sr fraction *x* in the precursor (b and d). For details about the Rietveld refinement, and discussions about the results, see the main text.

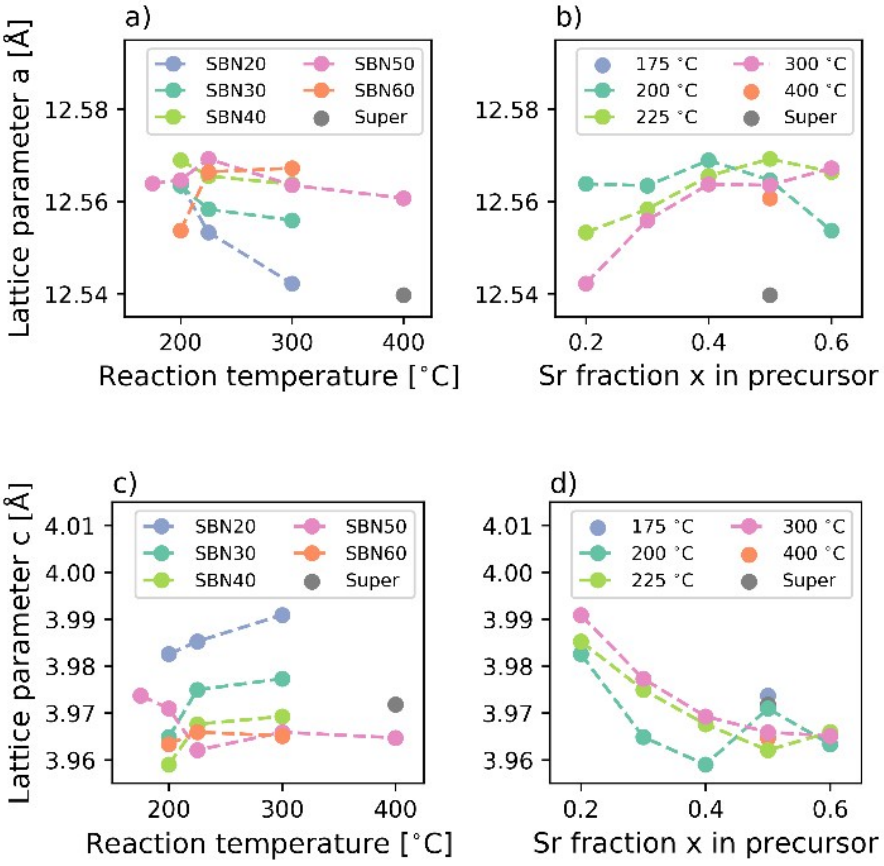

Figure S6:. Lattice parameters *a* (Figure a and b) and *c* (Figure c and d) from Rietveld refinement at the end of the experiments as a function of reaction temperature (Figure a and c) and Sr fraction x in precursor (Figure b and d)

Morphology development as a function of temperature and Sr fraction

Decreasing reaction time gives in general an increase in aspect ratio. At lower temperatures more compositions show signs of hollow cubes or rods, while SBN have tube shaped particles for all temperatures.

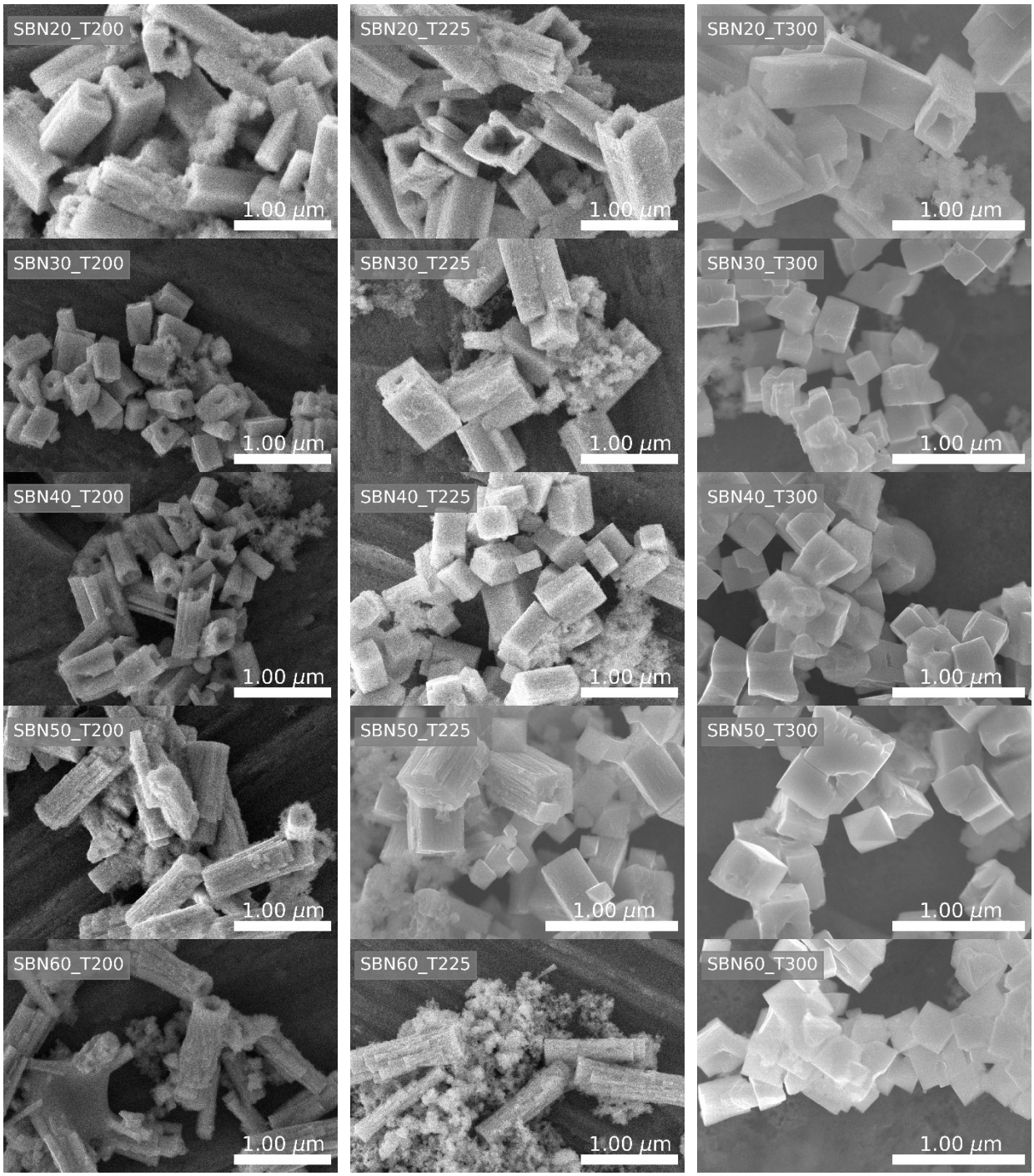

Figure S7: SEM images of all compositions (SBN20-60) with reaction temperatures of 200, 225 and 300 °C.

Summary of the final refined values for all experiments

Scale factor, isotropic Lorentzian and Guassian strain, lattice parameter, Sr fraction, Sr occupancy on A1-site, B_{iso} for the Nb1-, Nb2-, A1- and A2-site, and two atomic position parameters for the Nb2-site (x and y) and one for the A1-site for SBN were refined. Scale factor was refined for Pyro (with Pawley fit) and Uknw (with single peak phases) when present for the batch refinement, keeping lattice parameters (Pyro) and peak positions (Uknw) fixed to the values refined in the last frame.

Table S2: Refined values (strain, lattice parameter a and c, Sr fraction, Sr occupancy on A1-site, atomic displacement parameters for Nb1, Nb2, A1 and A2, atomic position parameters, R_{wp} and R_{bragg}) for the last frame from each experiment. Estimated standard deviations from *TOPAS* are given, where for example 1.5(1) equals 1.5 ± 0.1.

Sample	Strain [10^{-3}]	Lattice parameter a [Å]	Lattice parameter c [Å]	Sr fraction x [a.u.]	Sr occ A1 [a.u.]	Biso Nb1 [Å^2]	Biso Nb2 [Å^2]	x Nb2-site
SBN60_T300	0.76(2)	12.5672(2)	3.9651(1)	0.30(1)	0.75(1)	2.9(1)	2.0(1)	0.0751(2)
SBN60_T225	0.70(4)	12.5664(2)	3.9659(1)	0.38(2)	0.91(2)	3.3(2)	2.0(1)	0.0746(3)
SBN60_T200	0.75(5)	12.5537(3)	3.9633(2)	0.37(2)	0.92(3)	2.9(2)	2.3(1)	0.0744(4)
SBN50_T400	0.77(2)	12.5607(1)	3.9647(1)	0.34(1)	0.85(1)	2.4(1)	1.9(1)	0.0740(2)
SBN50_T300	0.66(1)	12.5635(1)	3.9659(1)	0.32(1)	0.81(1)	3.0(1)	2.13(5)	0.0746(2)
SBN50_T225	0.71(2)	12.5692(2)	3.9621(1)	0.33(1)	0.82(1)	3.4(1)	1.9(1)	0.0747(2)
SBN50_T200	0.71(2)	12.5644(2)	3.9710(1)	0.46(1)	0.86(1)	3.6(1)	2.2(1)	0.0730(2)
SBN50_T175	0.61(2)	12.5639(1)	3.9737(1)	0.41(1)	0.88(1)	3.7(1)	2.1(1)	0.0739(2)
SBN40_T300	0.60(1)	12.5637(1)	3.9693(1)	0.31(1)	0.77(1)	3.2(1)	2.18(4)	0.0740(1)
SBN40_T225	0.66(2)	12.5655(1)	3.9676(1)	0.37(1)	0.89(1)	3.4(1)	2.0(1)	0.0733(2)
SBN40_T200	0.62(2)	12.5689(1)	3.9590(1)	0.27(1)	0.66(1)	3.5(1)	2.3(1)	0.0745(2)
SBN30_T300	0.44(1)	12.5559(1)	3.9773(1)	0.24(1)	0.61(1)	3.3(1)	2.50(5)	0.0742(1)
SBN30_T225	0.55(1)	12.5583(1)	3.9749(1)	0.29(1)	0.73(1)	3.3(1)	2.4(1)	0.0736(2)
SBN30_T200	0.59(1)	12.5634(1)	3.9649(1)	0.26(1)	0.65(1)	3.4(1)	2.3(1)	0.0742(1)
SBN20_T300	0.78(2)	12.5422(2)	3.9909(1)	0.23(1)	0.57(1)	2.9(1)	2.3(1)	0.0736(2)
SBN20_T225	0.83(3)	12.5533(2)	3.9852(1)	0.24(2)	0.61(2)	3.0(2)	2.3(1)	0.0737(3)
SBN20_T200	0.73(3)	12.5638(2)	3.9826(1)	0.25(2)	0.62(2)	2.8(2)	2.7(1)	0.0743(3)
SBN50_supercrit	0.96(5)	12.5397(3)	3.9718(2)	0.60(2)	0.72(2)	3.1(2)	2.0(1)	0.0723(3)

Table S2 continued:

Sample	y Nb-site2	Biso A1-site [Å^2]	Biso A2-site [Å^2]	x A1-site	y A1-site	Occ vacancy A1 [a.u.]	R_{wp} [%]	R_{bragg} [%]	Beam time
SBN60_T300	0.2139(2)	0.0(2)	4.3(1)	0.1728(2)	0.6728(2)	0.50(2)	1.29	0.93	Feb
SBN60_T225	0.2132(3)	1.9(3)	4.3(2)	0.1736(4)	0.6736(4)	0.19(4)	1.63	0.83	Feb
SBN60_T200	0.2147(4)	0.8(4)	3.2(2)	0.1725(4)	0.6725(4)	0.16(1)	4.16	2.13	Oct
SBN50_T400	0.2131(2)	1.9(2)	3.8(1)	0.1732(2)	0.6732(2)	0.29(2)	1.63	0.85	Feb
SBN50_T300	0.2135(2)	1.0(2)	4.3(1)	0.1730(2)	0.6730(2)	0.39(2)	1.66	1.09	Feb
SBN50_T225	0.2132(3)	0.7(2)	4.7(1)	0.1720(3)	0.6720(3)	0.35(3)	2.25	1.35	Feb
SBN50_T200	0.2128(2)	1.8(2)	4.3(1)	0.1744(2)	0.6744(2)	0.29(3)	2.14	1.89	Feb
SBN50_T175	0.2126(2)	1.4(2)	3.7(1)	0.1739(2)	0.6739(2)	0.23(2)	1.67	1.23	Feb
SBN40_T300	0.2133(1)	0.9(1)	4.3(1)	0.1731(1)	0.6731(1)	0.45(2)	1.94	1.61	Feb

SBN40_T225	0.2132(2)	2.1(2)	4.4(1)	0.1736(2)	0.6736(2)	0.23(3)	1.90	1.47	Feb
SBN40_T200	0.2144(2)	0.0(2)	4.7(1)	0.1725(2)	0.6725(2)	0.67(2)	3.12	3.05	Oct
SBN30_T300	0.2130(1)	0.0(2)	4.3(1)	0.1729(1)	0.6729(1)	0.79(2)	2.37	2.35	Oct
SBN30_T225	0.2132(2)	1.0(2)	4.3(1)	0.1735(2)	0.6735(2)	0.53(2)	2.43	1.75	Oct
SBN30_T200	0.2134(2)	0.0(2)	4.5(1)	0.1727(1)	0.6727(1)	0.70(2)	4.15	3.31	Oct
SBN20_T300	0.2109(2)	0.0(3)	3.9(1)	0.1734(2)	0.6734(1)	0.85(2)	2.95	1.80	Oct
SBN20_T225	0.2169(3)	0.0(3)	4.3(1)	0.1732(3)	0.6732(3)	0.78(3)	6.74	3.62	Oct
SBN20_T200	0.2130(3)	0.0(3)	4.0(1)	0.1730(3)	0.6730(3)	0.76(3)	5.77	3.63	Oct
SBN50_supercrit	0.2092(3)	1.7(4)	2.8(2)	0.1732(3)	0.6732(3)	0.57(4)	4.56	2.95	Feb

Effect of changing the alkaline earth to niobium ratio in the Rietveld refinement

To determine the effect of non-stoichiometry (having the sum of alkaline earth higher or lower than the stoichiometric value of 5) on the Rietveld refinement, the last frame of SBN30_T300 was refined with varying amounts of alkaline earth (4.5 – 5.6). No other changes were done compared to the other refinements explained in the main text.

The results show that the B_{iso} value of the A1-site is 0 (nonphysical) for a total sum of 5 and less, and flattens out at 2.3 Å^2 for values higher than 5.4. Both R-values, R_{wp} and R_{bragg} decrease (which indicates an improved fit to the experimental data) with an increasing amount of Sr plus Ba. These results point towards a higher amount of alkaline earth than the stoichiometric value of 5 for the formed SBN.

Hypothetical charge compensation for an alkaline earth amount > 5 could be oxygen interstitials or free/itinerant electrons. Interstitial oxygen is unlikely, just as for perovskites, since the anion sublattice is close packed. Itinerant electrons have been suggested at the charge compensation in $Sr_{1.2-x}Ba_xNb_2O_6$ (filled SBN, with 6 alkali earth) made under reducing conditions [4].

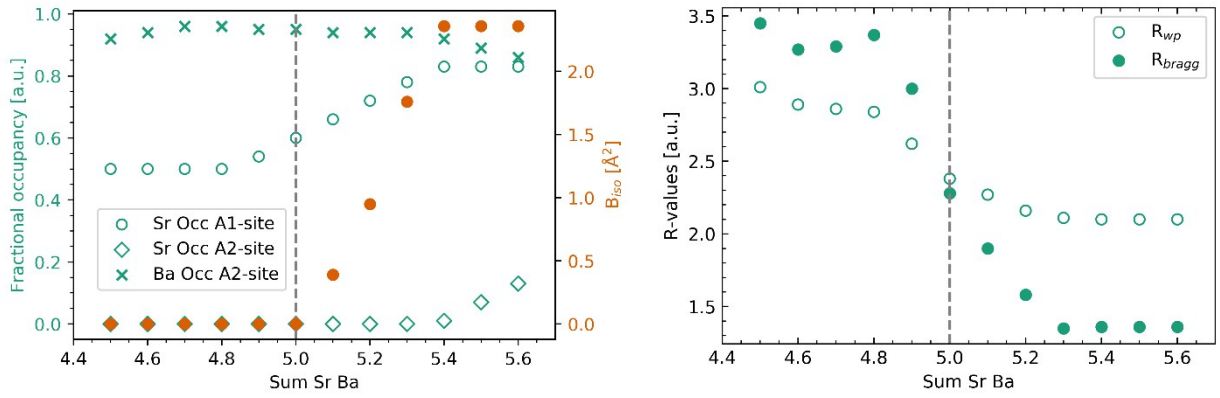

Figure S8: Refined values for Sr occupancy on the A1- and A2-sites, Ba occupancy on the A2-site and B_{iso} value for the A1-site (left) and the corresponding R_{wp} and R_{bragg} values as a function of sum of amount of alkaline earth included in the Rietveld refinement. Grey line indicates the stoichiometric amount for the sum of alkaline earth.

References

1. Carrio, J.G.; Mascarenhas, Y.P.; Yelon, W.; Santos, I.A.; Garcia, D.; Eiras, J.A. Structure Refinement of (Sr,Ba)Nb_2O_6 Ceramic Powder from Neutron and X-Rays Diffraction Data. *Mater. Res.* **2002**, *5*, 57-62.
2. Aamlid, S.S.; Selbach, M.S.; Grande, T. The Effect of Cation Disorder on Ferroelectric Properties of $Sr_xBa_{1-x}Nb_2O_6$ Tungsten Bronzes. *Materials* **2019**, *12*; doi:10.3390/ma12071156.
3. Podlozhenov, S.; Graetsch, H.A.; Schneider, J.; Ulex, M.; Wohlecke, M.; Betzler, K. Structure of strontium barium niobate $Sr_xBa_{1-x}Nb_2O_6$ (SBN) in the composition range 0.32 <= x <= 0.82. *Acta Crystallogr. Sect. B* **2006**, *62*, 960-965; doi:doi:10.1107/S0108768106038869.
4. Kolodiazhnyi, T.; Sakurai, H.; Isobe, M.; Matsushita, Y.; Forbes, S.; Mozharivskyj, Y.; Munsie, T.J.S.; Luke, G.M.; Gurak, M.; Clarke, D.R. Superconductivity and crystal structural origins of the metal-insulator transition in $Ba_{6-x}Sr_xNb_{10}O_{30}$ tetragonal tungsten bronzes. *Phys. Rev. B* **2015**, *92*, 214508; doi:10.1103/PhysRevB.92.214508.